universität innsbruck

Experiment E118 - Gaussian Beams and Optical Resonators

Robin Hoffmann[*], Arik Bürkle[†], Valentin Ertl[‡]

June 10, 2025

Abstract

In this experiment, we employed lasers and optical resonators to characterize the beam profile of a Gaussian laser mode. Initially, we measured the width of the laser beam at various distances from the laser source. Our findings indicated that the origin of the laser is positioned at 220,2(14) µm from the lens output, with a width of −16,01(12) cm. Subsequently, we conducted a spectral analysis of the laser modes.

[*]robin.hoffmann@student.uibk.ac.at
[†]arik.buerkle@Student.uibk.ac.at
[‡]valentin.ertl@student.uibk.ac.at

Contents

1 Introduction

Gaussian beams and optical resonators play an important role in this experiment. Gaussian beams are a fundamental concept in the field of optics and photonics, representing a type of electromagnetic wave that maintains a Gaussian intensity profile as it propagates through space. These beams are solutions to the paraxial approximation of the Helmholtz equation [1], making them essential for understanding the behavior of light in various optical systems. The Gaussian beam model is particularly valuable because it accurately describes the output of many laser systems, which typically emit light with a Gaussian intensity distribution [2]. Optical resonators, also known as optical cavities, are structures that confine and sustain electromagnetic waves by repeated reflection between mirrors. These resonators are pivotal components in laser technology, as they determine the spatial and spectral characteristics of the emitted laser light [3]. The interaction between Gaussian beams and optical resonators forms the basis of laser operation, where the resonator supports specific modes of the electromagnetic field that correspond to stable Gaussian beam solutions. Understanding Gaussian beams involves examining their properties such as beam waist, divergence, and the Rayleigh range, which describe how the beam evolves in free space [1]. When considering optical resonators, it is crucial to analyze parameters like the mirror curvature, separation distance, and the stability criterion, which influence the formation of resonant modes and the efficiency of light confinement. In this context, the study of Gaussian beams and optical resonators is not only critical for the design and optimization of lasers but also for applications in optical communication, microscopy, and various fields requiring precise control over light propagation and confinement [2][3]. This experiment is intended to provide a deeper exploration of the theoretical and practical aspects of Gaussian beams and optical resonators, emphasizing their significance in advancing modern optical technology.

2 Theory

In this section, we elucidate the fundamental physics governing laser beam propagation, the behavior of optical lenses, and the principles underlying optical resonators.

2.1 Gaussbeam

From the principles of electrodynamics, it is established that light manifests as the propagation of alternating electric and magnetic fields. These waves must adhere to Maxwell's equations, which yield various solutions contingent upon the system's symmetry. Among these solutions are the Helmholtz equations, which describe the behavior of electromagnetic fields propagating along a single axis. Solutions satisfying this condition are termed Gaussian modes ($U_{(m,n)}(x,y,z)$), where x, y, and z represent spatial coordinates, and (m,n) denotes the transverse mode indices. For the (0,0) index, the resultant solution corresponds to a Gaussian beam as defined by the equation: 1.

$$U_{(0,0)}(x,y,z) = A_0 \frac{w_0}{w(z)} \cdot exp\left(\frac{-(x^2+y^2)}{w(z)^2}\right) \cdot exp\left(-ikz - ik\frac{x^2+y^2}{2R(z)} + i\Phi(z)\right) \tag{1}$$

With A_0 representing the amplitude of the wave, w_0 denoting the minimum radius of the beam, $w(z)$ as the radius at position z, k being the wave vector, $R(z)$ signifying the curvature at position z, and $\Phi(z)$ describing the phase propagation, the intensity of light at a given position (x,y,z) is directly proportional to the squared absolute value of the wave, expressed as $I \sim |U|^2$. Consequently, this yields an intensity distribution as defined by Equation 2, where I_0 represents the maximal intensity.

$$I = I_0 \left(\frac{w_0}{w(z)}\right)^2 \cdot exp\left(\frac{-2(x^2+y^2)}{w(z)^2}\right) \tag{2}$$

The significant characteristic of this Gaussian beam is its divergence as the beam extends farther from its origin point. This divergence results in a variation in the beam radius along the z-axis, described by Equation 3.

$$w(z) = w_0 \sqrt{1 + \left(\frac{z}{z_R}\right)^2} \tag{3}$$

The parameter z_R represents the Rayleigh length, indicating the point at which the beam radius is $\sqrt{2}$ times the original radius w_0. This length is contingent upon the wavelength of the laser, expressed as $z_R = \pi w_0^2/\lambda$. It serves as a basis for two distinct approximations: the far-field regime ($|z| \gg z_R$) and the near-field regime ($|z| \ll z_R$).

In the far-field regime, the Gaussian beam can be conceptualized as a spherical wave originating from a single point in space. Conversely, in the near-field regime, the wave can be approximated as a plane wave propagating in the x-direction. This behavior is illustrated in Figure 1, where the wavefronts bulge as z increases, yet remain planar for small z-values. The bulging effect is characterized by the curvature of the wave, $R(z)$, as defined by Equation 4.

$$R(z) = z\left(1 + \left(\frac{z_r}{z}\right)^2\right) \tag{4}$$

A curvature of $R(z) \sim \infty$ defines a flat curve, while $R(z) \sim z$ approximates a spherical wave.

In the far-field regime, the equations can be simplified to 5.

$$w(z) \simeq w_0 \frac{z}{z_R} = \theta z \tag{5}$$

where $\theta \simeq \lambda/(\pi w_0)$ represents the divergence angle of the beam. All these properties are illustrated in Figure 1, depicting the divergence of a Gaussian beam as a function of z in the x-y plane.

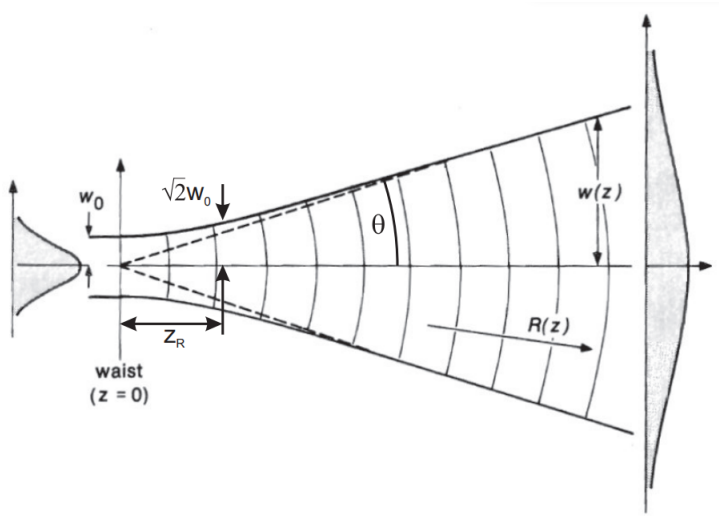

Figure 1: The diagram illustrates a Gaussian beam propagating along the z-axis, depicted as a cross-section in the x-y plane. Key features annotated in the diagram include: w_0, the beam waist radius at position z_0; z_R, the Rayleigh range, where the beam radius expands to $\sqrt{2}w_0$; θ, the divergence angle of the far-field; and the curvature and radius of the wavefront at an arbitrary position z. [1]

2.2 Focusing with lenses

The description of a laser beam propagating through lenses or other optical elements is often achieved using a complex beam parameter $q(z)$:

$$\frac{1}{q(z)} = \frac{1}{R(z)} - i\frac{\lambda}{\pi w(z)^2} \tag{6}$$

Here, $R(z)$ represents the radius of curvature of the wavefront, and $w(z)$ is the beam radius. λ denotes the wavelength of the light. This parameter $q(z)$ enables efficient analysis and calculation of beam properties as it passes through optical systems.

When a laser beam described by $q_1(z)$ is transformed by passing through an optical element, the new beam parameter $q_2(z)$ can be calculated using the ABCD matrix formalism:

$$\frac{1}{q_2} = \frac{C + D/q_1}{A + B/q_1} \tag{7}$$

The matrix parameters A, B, C and D characterize the optical element and are components of the ABCD matrix:

$$\begin{pmatrix} A & B \\ C & D \end{pmatrix} \tag{8}$$

This formalism allows for straightforward computation of the beam's evolution through a series of optical elements by multiplying the respective ABCD matrices. The order of matrix multiplication corresponds to the order in which the beam traverses the optical elements (from right to left).

For a lens with focal length f and a collimated beam (radius of curvature $R_1 = \infty$) with an initial beam radius w_1, the beam radius w_2 at the focus of the lens is given by:

$$w_2 = \frac{\lambda f}{\pi w_1} \tag{9}$$

Figure 2 shows this concept schematically.

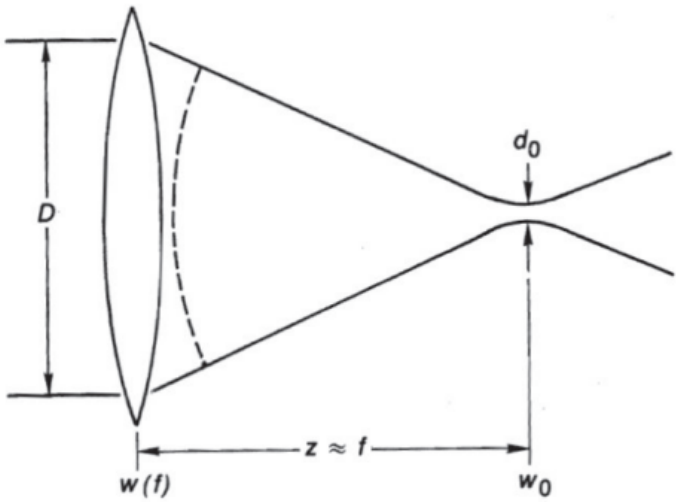

Figure 2: Beam focus of a collimated Gaussian beam after passing through a lens. [1]

The ability to control the beam radius and focal position using lenses is one of the fundamental tasks in optics. The ABCD matrix formalism offers an elegant method for calculating beam parameters after passing through complex optical systems. In addition to analytical methods, modern software toolboxes, such as LightMachinery [4], are available to perform these calculations.

2.3 Optical resonators

Optical resonators are fundamental components in modern optics, essential for lasers and various spectroscopic applications. They consist of mirrors arranged to reflect a light beam multiple times along the same path, enhancing certain wavelengths and forming standing waves like illustrated in Figure 3.

The simplest form of an optical resonator uses two parallel mirrors. Standing waves form between these mirrors, with nodes at the mirror surfaces. The distance between successive resonance frequencies is called the free spectral range (FSR):

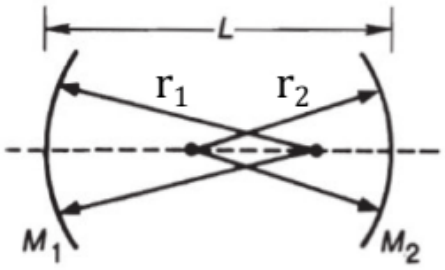

Figure 3: Schematic representation of an optical resonator. The configuration includes two mirrors that reflect the light beam back and forth and form standing waves. The device ensures that only certain wavelengths resonate within the resonator cavity, which are determined by the distance L between the mirrors and their curvature r. [1]

$$\mathrm{FSR} = \frac{c}{2L} \tag{10}$$

where c is the speed of light and L is the distance between the mirrors.
Gaussian beams, which expand in diameter with distance, require curved mirrors to remain confined within the resonator. For mirrors with equal curvature radius r and separation d, the beam waist w_0 necessary for coupling is given by:

$$w_0 = \sqrt{\frac{d(2r-d)}{2}} \tag{11}$$

2.3.1 Stability and Spectral Properties

Resonator stability depends on the mirror curvature r_1, r_2 and the separation d. The stability criterion is:

$$0 \leq g_1 g_2 \leq 1 \quad \text{with} \quad g_{1,2} = 1 - \frac{d}{r_{1,2}} \tag{12}$$

The transmission spectrum of a TEM_{00} mode shows peaks separated by the FSR, with a bandwidth $\Delta\nu$. The finesse F, defined as:

$$F = \frac{\mathrm{FSR}}{\Delta\nu} \tag{13}$$

indicates the sharpness of the resonance peaks.

2.3.2 Mode Matching

For optimal coupling, the laser beam waist must match the resonator mode waist. In a symmetric resonator (with $r_1 = r_2 = r$), the mode waist is determined by:

$$2z_R = \sqrt{L(2r-L)} \tag{14}$$

2.3.3 Higher Order Modes

If mode matching is imperfect, higher-order modes (TEM_{mn}) may be excited. These modes are described by:

$$U_{mn} \sim U_{00} H_m \left(\sqrt{2} \frac{x}{w(z)} \right) H_n \left(\sqrt{2} \frac{y}{w(z)} \right) \tag{15}$$

where H_m and H_n are Hermite polynomials. The resonance condition for these modes is:

$$\nu_{qmn} = \left(q + 1 + \frac{m + n + 1}{\pi} \arccos \left(1 - \frac{L}{r} \right) \right) \Delta\nu_{\mathrm{FSR}} \tag{16}$$

3 Experiment setup and execution

The following text sections illustrate the experimental setup and explain the exact data recording and execution of the experiment.

3.1 Experiment setup

The experimental setup was set up in the practical room as shown in Figure 4. A helium-neon laser (1) with a wavelength of $\lambda = 632.8$ nm was used for the experiment. The beam path of the laser is indicated by the red line in 4. Immediately after the laser, an optical isolator (2) is placed to avoid back reflections. Object 3 in the picture shows the waistmeter with which the beam diameter of the laser beam can be determined. But more on this in section 3.2. The measuring head of the waistmeter consists of a photodiode which is periodically covered by a rotating blade. Care must be taken to ensure that the laser beam falls vertically onto the photodiode to keep the error in the beam diameter measurement as low as possible. An electronic system uses the photodiode signal to calculate the beam diameter. The value of the calculated beam diameter is displayed on this system which can be seen to the right of the waistmeter (3). After the laser beam has left the isolator, it is deflected by two mirrors (4) so that it hits the optical resonator, which consists of two curved mirrors (6 and 7) with a radius of $r_{1,2} = 150$ mm and a reflectivity of $R \approx 98\%$. A piezo crystal is located before the first mirror (6) to create different modes. This is possible because a function generator sends a signal to a high-voltage amplifier, which in turn is connected to the piezo. The position of the second mirror can be changed using a micrometerscrew. The beam also passes through the 200 mm focusing lens (5) beforehand. At the end, the laser beam hits the photodiode (8), which is used to measure the radiation intensity and which is coupled to an oscilloscope in order to be able to evaluate the photodiode signal. This enabled us to see TEM-modes of a Gaussian beam and to capture the images with a camera, which is not shown in figure 4. [1]

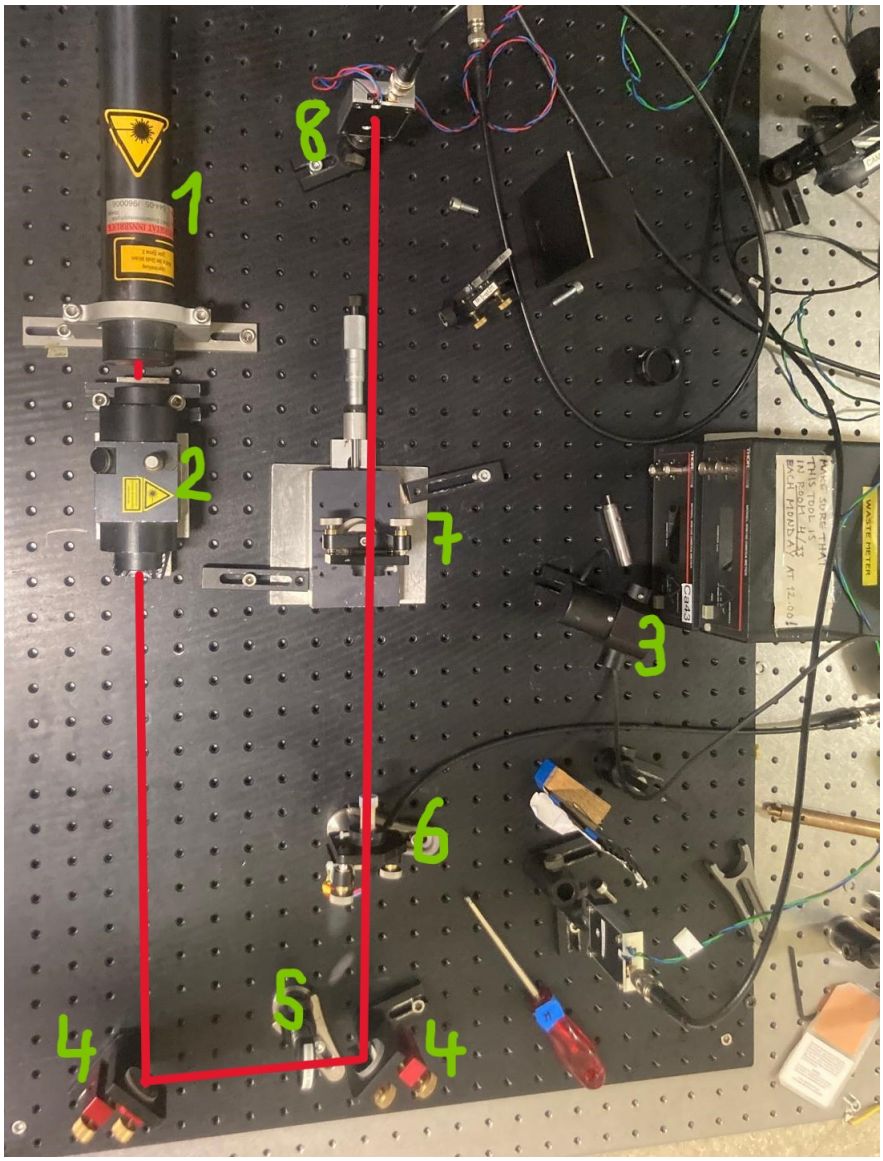

Figure 4: Experimental setup how it was set up in the practical room. The numbers correspond to following items: helium-neon laser (1); optical isolator (2) to avoid back reflections; waistmeter with electronic system to measure the beam diameter (3); deflecting mirror (4); 200 mm focusing lens (5); optical resonator (6, 7) with curved mirrors and piezo in front of the first mirror (6); photodiode (8) to measure the radiation intensity.

3.2 Execution

In the first part of the experiment, the beam profile of the Gaussian beam emerging from the laser had to be completely determined. For this purpose, the beam diameter was measured at selected distances from the laser using the waistmeter and then the beam profile was determined by fitting the experimental data. More on this later in the data analysis, see section 4. In this part of the experiment we determine the minimal beam waist w_0 of the laser beam without a lens. In order to get the beam diameter depending on the distance z to the laser, we always note the distance to the laser z and the beam diameter w(z) corresponding to this distance. The beam diameter was then also measured in the same way at various selected points in the beam path after a 50 mm lens.

In the second part of the experiment we want to examine the behavior of a Gaussian Beam if we let it pass through an optical resonator. In preparation for this second part of the experiment, we first calculated the beam waist for the resonator used in the confocal configuration. All calculated values are of course given later in the data analysis. Then we had to adjust the mode of the HeNe laser to the resonator mode using a selection of lenses (f = 75 mm, 100 mm and 200 mm) without the resonator mirrors. We used the prepared values of the laser beam waist and the resonator waist to determine which, and how many, lenses were required. For this step we tried out the online toolbox "lightmachinery". Unfortunately, after a lot of trial and error, we still couldn't find the right lens and the right position. The internship supervisor then gave us the hint that it could only be the 200 mm lens and showed us the position where we should place it. To examine the behavior of a Gaussian Beam if we let it pass through an optical resonator, first we had to ensure that the laser beam hits one of the two mirrors centered after the beam passes through the lense. It is very important that the beam waist of the beam is located exactly between the two mirrors. This optical resonator respectively the piezo is connected to a high-voltage amplifier which allows us to change the length of the resonator and thus generate a wide variety of resonances. We than measured the beam intensity with a photodiode behind the resonator. The applied voltage respectively the frequency and the intensity were displayed on an oscilloscope. The setup was optimized by adjusting the resonator or the two mirrors in front of the resonator accordingly so that we can clearly see the TEM_{00} mode on the oscilloscope which has a higher amplitude than the rest of the modes. We then recorded various modes with the CCD camara. We obtained these higher order modes by slightly misaligning the coupled beam. Now the photodiode was set up again after the resonator and complete mode images were stored for a further mirror distance. The mode matching was deliberately not changed and a mode mismatch was therefore consciously accepted. [1]

4 Experimental results

In this section, we will characterize the radius profile of the laser used, calculate the focal radius for two different lenses, and analyze the resonant modes of the laser.

4.1 Characterisation of the laser and lenses.

In the first part of the experiment, we characterized the waist of the HeNe laser used. To do this, we placed a waist meter at different distances along the laser beam path to measure the beam diameter. The distance from the waist meter to the laser exit point was measured using a ruler, resulting in an uncertainty of 0,2 cm due to the smallest unit on the ruler being 0,1 cm and the difficulty of consistently finding the exact same location on the waist meter for each measurement.

Once the distance was measured, the diameter of the beam was read from the waist meter. The error in the diameter measurement reflects the variation observed while measuring. For small diameters, the values varied little, but for larger diameters, the variation increased. After collecting the measurements, we fit the data using Equation 3 to determine the minimum waist and its position along the z-axis.

The collected data and the fitting function are shown in Figure 5.

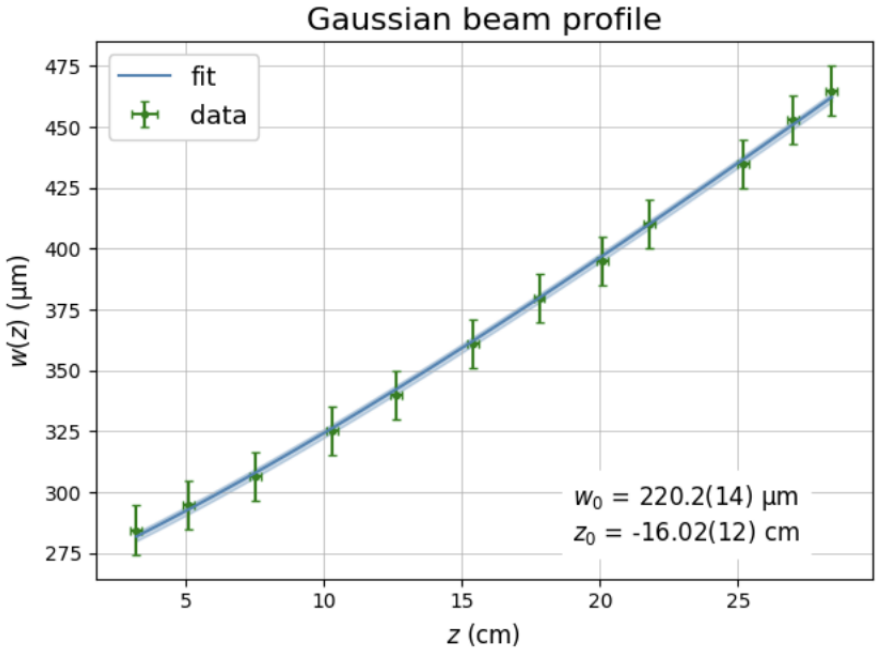

Figure 5: The diagram depicts the laser radius w as a function of distance from the laser output z. A fit has been applied to the data, described by function 3 with $w_0 = 220{,}2(14)\,\mu\text{m}$ and $z_0 = -16{,}02(12)\,\mu\text{m}$. The minimum of the fit function describes the waist w_0 and its associated distance point z_0.

From the fit function, we found that the laser originates at the point $-16{,}02(12)\,\text{cm}$ with a waist of $220{,}2(14)\,\mu\text{m}$. In the far field, the beam diverges with an angle of $0{,}915(6)\,\text{mrad}$.
Next, we introduced a lens into the beam path. Initially, we placed a lens at the position $z = 3{,}5(2)\,\text{cm}$ with a focal length of $f = 50\,\text{mm}$ and repeated the experiment to characterize the waist profile of the laser after the lens. This resulted in the following data set: 6. We found that the point where the laser has the smallest waist is at $z = 9{,}23(3)\,\text{cm}$ with a waist of $w_0 = 34{,}7(4)\,\mu\text{m}$. This result is consistent with the theoretical calculation for the waist from Equation 9, which predicts a waist of $35{,}5(2)\,\mu\text{m}$.

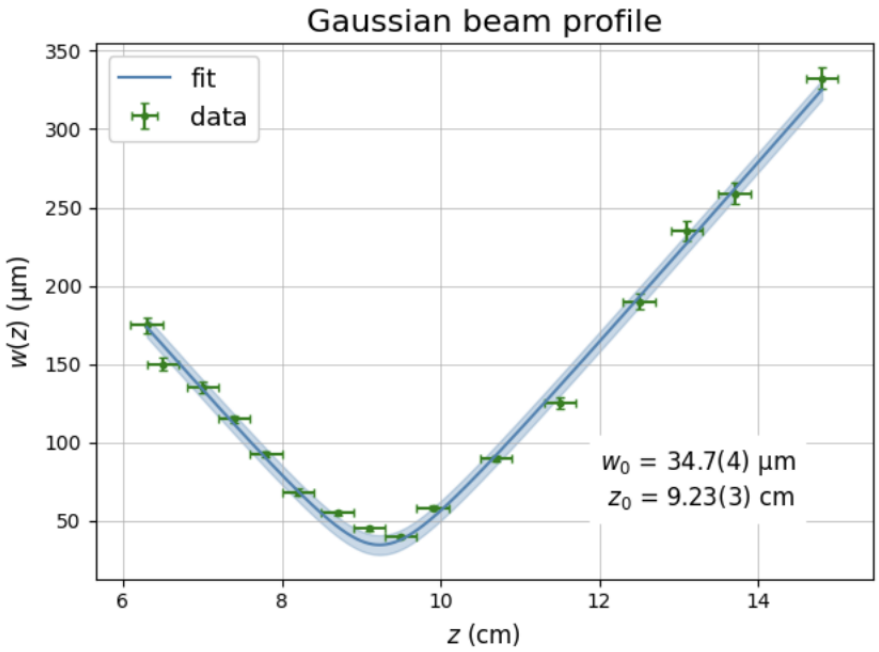

Figure 6: The diagram illustrates the laser radius w as a function of distance z from the laser output. This beam originates from a laser propagating through a lens with a focal length of $f = 50\,\text{nm}$. A fitting procedure has been applied to the data, described by Equation 3, where $w_0 = 34{,}7(4)\,\mu\text{m}$ and $z_0 = 9{,}23(3)\,\mu\text{m}$. The minimum of the fit function corresponds to the focal waist w_0 and its associated distance point z_0 from the lens.

Later in the experiment, we aimed to match the waist of the laser to the waist of the resonator. To achieve this, we placed a lens at $z = 46{,}5(5)\,\text{cm}$ with a focal length of $f = 200\,\text{mm}$ and conducted the same experiment for this lens one last time. We found the waist to be $88(2)\,\mu\text{m}$ and the focus position to be $z = 78{,}2(3)\,\text{cm}$, as shown in Figure 7.
Calculating the waist for the lens at that position, we found $w_0 = 65{,}76(14)\,\mu\text{m}$, which differs from the experimental results. This discrepancy could be due to systematic errors. One possible source of error is that the focal length of the lens might not be exactly 200 mm. Another potential source of error is the incorrect positioning of the lens, leading to a different beam radius upon entering the lens.A third reason for this mismatch is the fact that in Equation 9, we used the approximation that $f \gg z_R$. This is no longer the case for the 200 mm lens. This causes our calculated value for the waist to differ from the actual value. Despite these discrepancies, our direct measurement showed the beam radius to be $124{,}0(15)\,\mu\text{m}$, which is consistent with the required $w_1 = 123\,\mu\text{m}$ for the FSR. This matching of the waist is know as mode matching.

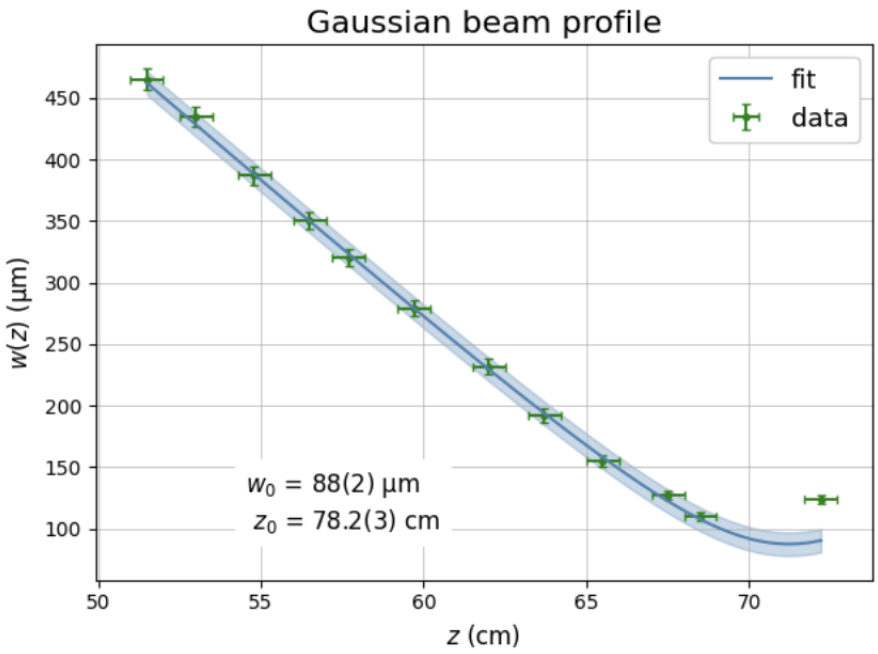

Figure 7: The diagram illustrates the laser radius w as a function of distance z from the laser output. This beam originates from a laser propagating through a lens with a focal length of $f = 200\,\text{nm}$. A fitting procedure has been applied to the data, described by Equation 3, where $w_0 = 88(2)\,\mu\text{m}$ and $z_0 = 78{,}2(3)\,\mu\text{m}$. The minimum of the fit function corresponds to the focal waist w_0 and its associated distance point z_0 from the lens.

4.2 Spectral and spatial analysis of the laser

To analyze the different modes of the laser, we directed the beam into a resonator equipped with a piezo crystal. The precise length of the resonator allows us to filter the modes that are resonant within it. By applying a rising voltage to the piezo crystal, we can slightly alter the resonant condition to scan the frequency spectrum. This scan enables us to adjust the resonator length to find positions where only the TEM_{00} mode passes through, where both the TEM_{00} and TEM_{10} modes pass through, and where multiple modes are present.

Using a CCD camera, we captured images of the different mode combinations. By comparing these images with a theoretical diagram (Figure 11), we observed that the first and second images correspond to the TEM_{00} and TEM_{10} modes, respectively. The last image does not match any single mode, indicating it is an overlap of different modes.

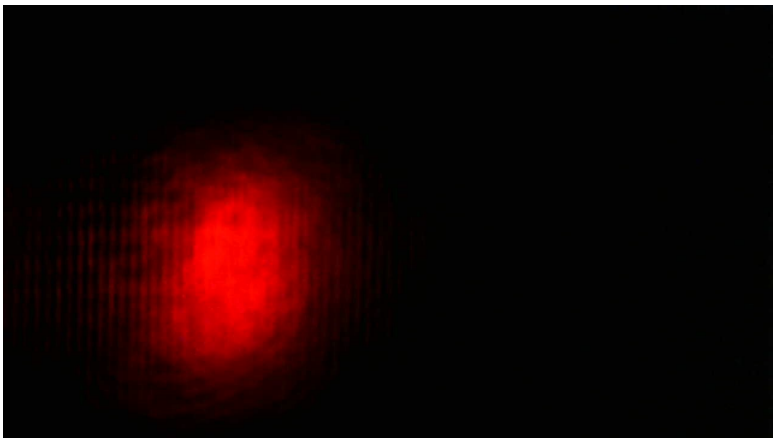

Figure 8: The figure displays the capture of the TEM_{00} laser mode.

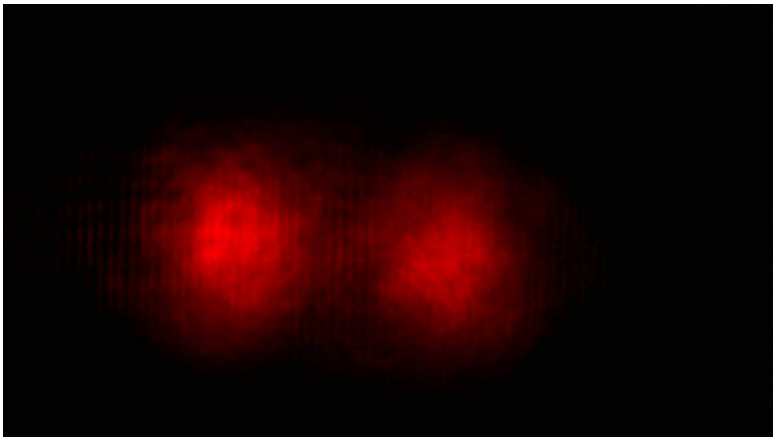

Figure 9: The figure displays the capture of the TEM_{10} laser mode.

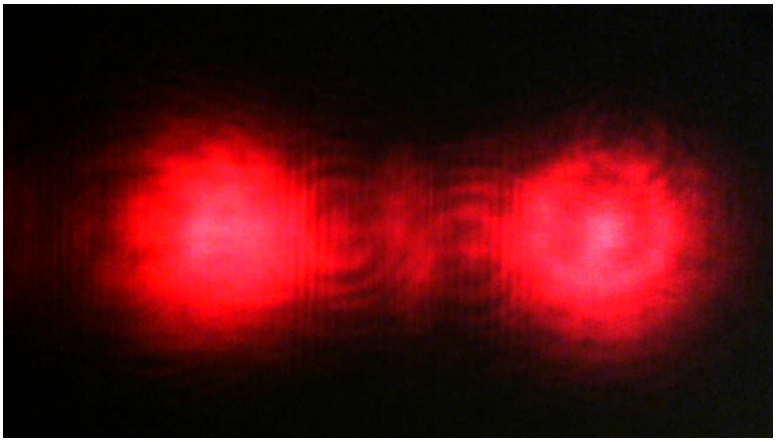

Figure 10: The figure displays the capture of a combination of higher order laser modes.

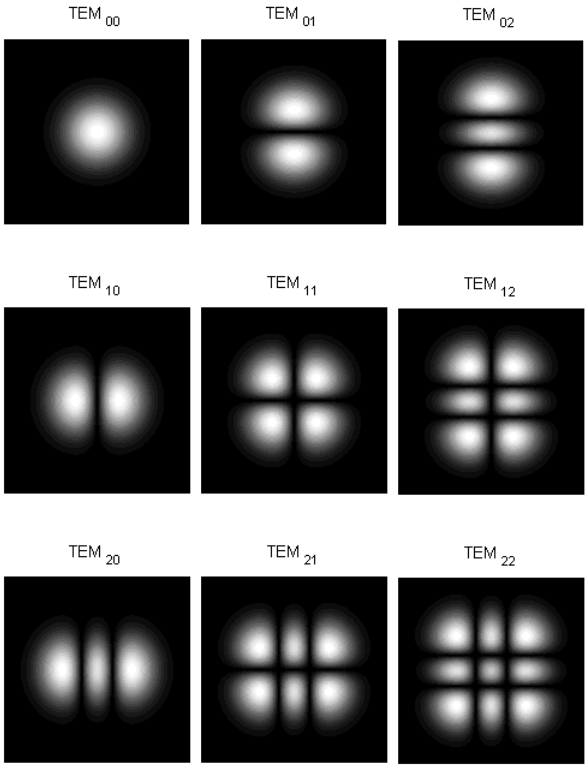

Figure 11: The thoratical spatial resolution of different TEM modes of the Laser. [5]

The second part of this experiment entailed spectral analysis. We utilized a photodiode to track the laser intensity over time. By modulating the resonator's length through voltage adjustments, we could alter its resonant frequency, facilitating a spectral examination of the laser light. The separation between two spectral peaks signifies the resonator's free spectral range (FSR), measured at 406(4) MHz.

For the initial resonator length, where solely the TEM_{00} mode is observable, we acquired the subsequent spectrum: To analyze a single spectrum, we zoomed in on a specific peak and con-

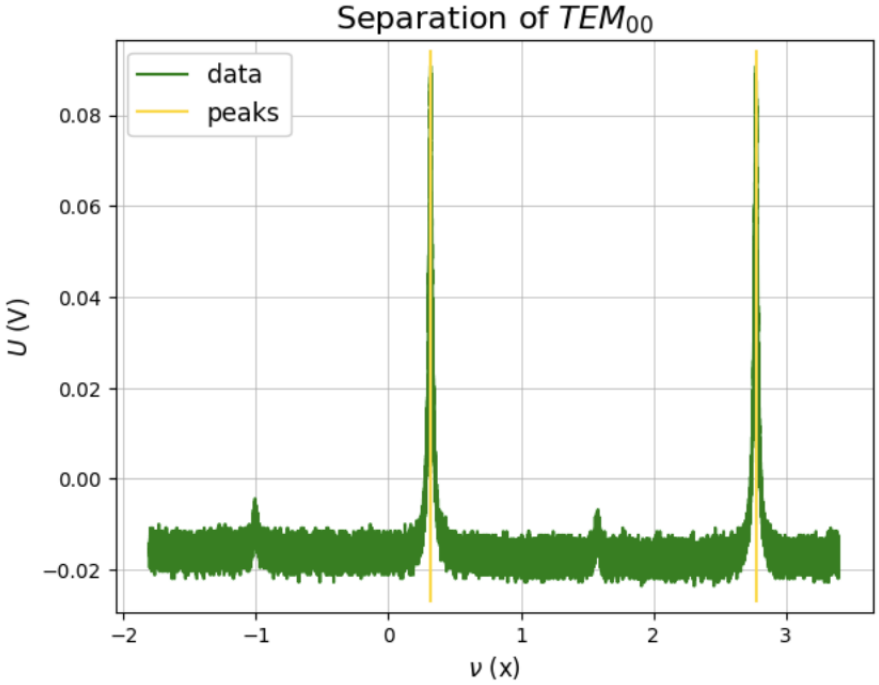

Figure 12: The diagram illustrates the oscilloscope output, plotting the voltage U generated by the TEM_{00} laser mode on the photodiode against time, with the time unit being arbitrary. We are currently scrutinizing a larger segment of the signal to identify the individual peaks and subsequently determine the free spectral range (FSR) $\Delta\nu_{FSR} = 2{,}456\,33(3)$ x

ducted a Lorentzian fit to that peak, as depicted in Figure 13. From this analysis, we determined a finesse of $F = 28{,}55(2)$. The error associated with this finesse is relatively low, likely underestimated. This is because we only examined one FSR and one peak for analysis. In reality, the data would vary across multiple measurements, resulting in errors associated with the standard deviation of the mean value for the data.

For the second setup, we conducted the same spectral analysis, resulting in Figure 14. We observe a second smaller peak in the spectrum, representing the TEM_{10} mode. This peak should ideally be located in the middle of the FSR; here, it is very close to the FSR's midpoint. Zooming in again on the TEM_{10} peak, we can perform a second fit, which may yield a smaller amplitude. Lastly, we conducted a spectral analysis of multiple modes, as shown in Figure 16, where we observe multiple overlapping modes.

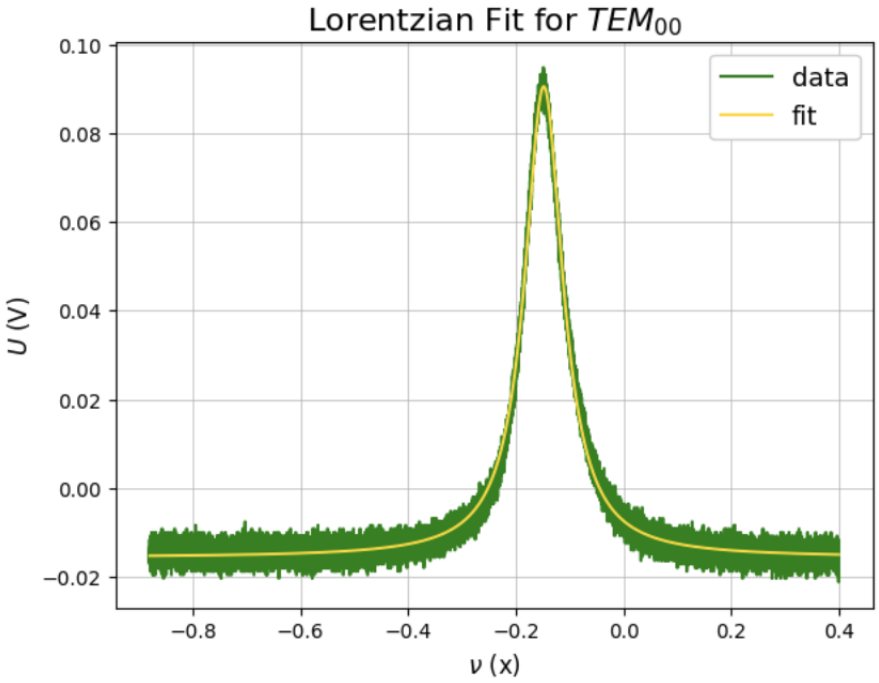

Figure 13: The diagram depicts the output of the oscilloscope, where the voltage U generated by the TEM_{00} laser mode on the photodiode is plotted against time, with the time unit being arbitrary. A Lorentzian fit has been applied to the signal, yielding the full width at half maximum (FWHM) $\Delta\nu = 0{,}086\,03(7)$ x.

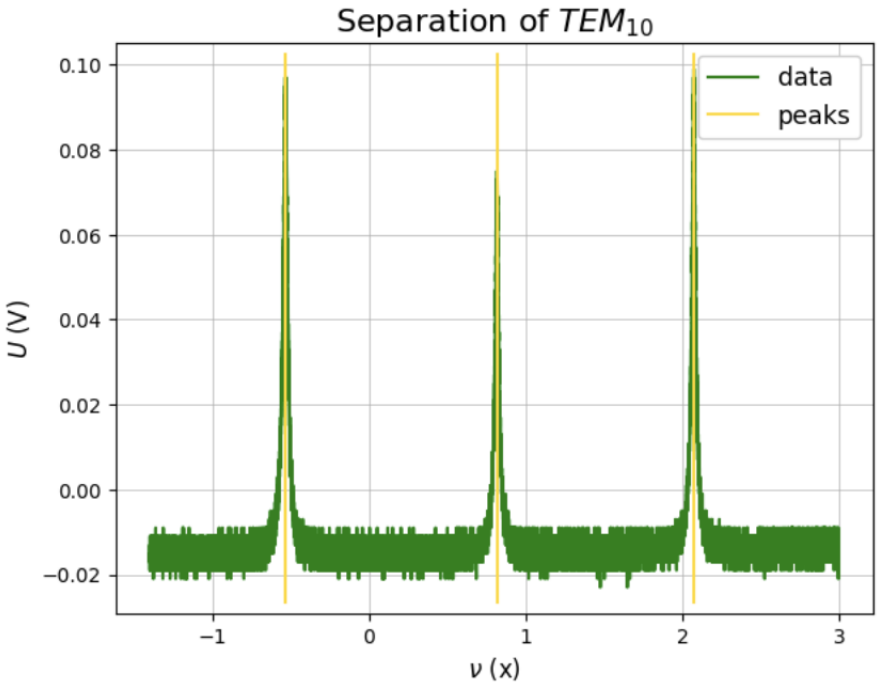

Figure 14: The diagram illustrates the oscilloscope output, plotting the voltage U generated by the TEM_{10} laser mode on the photodiode against time, with the time unit being arbitrary. We are currently scrutinizing a larger segment of the signal to identify the individual peaks and subsequently determine the free spectral range (FSR) $\Delta\nu_{FSR} = 2{,}607\,95(3)$ x. The relative separations between the secondary peaks are determined to $\Delta\nu_{12} = 0{,}518\,180(13)\,\Delta\nu_{\mathrm{FSR}}$ and $\Delta\nu_{23} = 0{,}481\,820(13)\,\Delta\nu_{\mathrm{FSR}}$

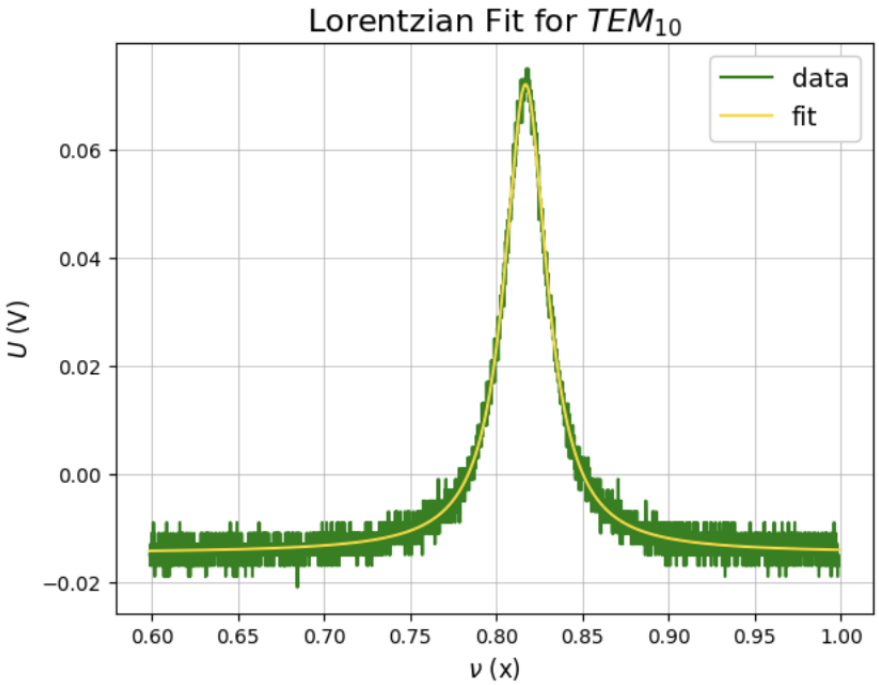

Figure 15: The diagram depicts the output of the oscilloscope, where the voltage U generated by the TEM_{10} laser mode on the photodiode is plotted against time, with the time unit being arbitrary. A Lorentzian fit has been applied to the signal, yielding the full width at half maximum (FWHM) $\Delta\nu = 0{,}029\,95(8)\,\mathrm{x}$.

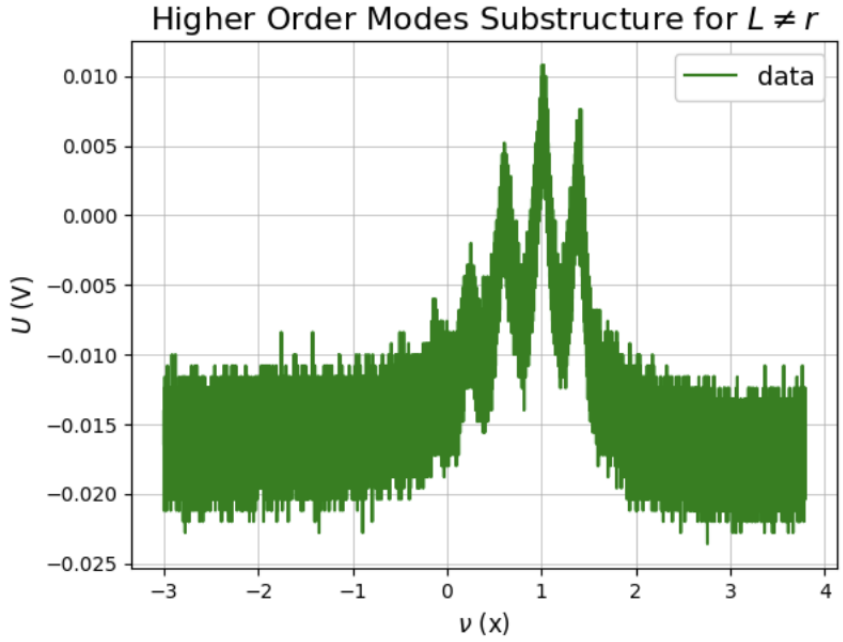

Figure 16: The diagram illustrates the oscilloscope output, plotting the voltage U generated by a combination of higher order laser modes on the photodiode against time, with the time unit being arbitrary.

5 Discussion

In this experiment, we analyzed the Gaussian laser beam to gain a better understanding of laser operation. Firstly, we characterized the waist of the laser to be $w_0 = 220{,}2(14)\,\mu\text{m}$ at the position $z_0 = -16{,}01(12)\,\text{cm}$. Subsequently, we investigated the different modes of the laser using a resonator. From this analysis, we demonstrated that different laser modes overlap after the resonator if it is detuned from its lens radius. We were able to characterize the spectra of the modes using Lorentzian fits and calculated the finesse of the resonator to be $F = 28{,}55(2)$.

References

[1] U. Innsbruck. *Gaussian beams and optical resonators*. Skript; retrieved on 14.05.24.

[2] Wikipedia. *Gaussian beam*. Online; Status 22.05.24. Retrieved on 23.05.24. URL: https://en.wikipedia.org/wiki/Gaussian_beam.

[3] Wikipedia. *Optical cavity*. Online; Status 07.01.24. Retrieved on 23.05.24. URL: https://en.wikipedia.org/wiki/Gaussian_beam.

[4] LightMachinery. *Gaussian Beam Propagation*. Online; Retrieved on 23.05.24. URL: https://lightmachinery.com/optical-design-center/gaussian-beam-propagation/.

[5] Wikipedia. *Different intensity profiles for a resonator with rectangular mirrors*. Online; Status 13.09.06. Retrieved on 23.05.24. URL: https://de.wikipedia.org/wiki/Laser#/media/Datei:TEMmn.png.

Explenation

Hereby we confirm that the present report was written independently and that all necessary sources and references have been provided.

Arik Bürkle	23.05.2024
Student 1	Date
Robin Hoffmann	23.05.2024
Student 2	Date
Valentin Ertl	23.05.2024
Student 3	Date

Arbeitsaufwand

Arik Bürkle
Vorbereitung:4h
Versuch:4h
Bericht:13h
Robin Hoffmann
Vorbereitung:3h
Versuch:4h
Bericht:12h
Valentin Ertl
Vorbereitung:3,5h
Versuch:4h
Bericht:8h

Looking back, it can be said that this experiment was completely terrible. There was far too little time and explanation during the experiment, and the script did not allow us to solve all the required tasks. However, we think we were not the problem of this experiment. The experiment should be revised or better explained. The setup of the experiment alone is frustrating enough, not to mention the data analysis, which requires far too much time. We were able to determine some of the required values, with which you will now have to be satisfied. Adding an additional "voluntary" bonus task at the end is simply ridiculous.